Improving Cutaneous Scar by Controlling the Mechanical Environment

Large Animal and Phase I Studies

Geoffrey C. Gurtner, MD,* Reinhold H. Dauskardt, PhD,† Victor W. Wong, MD,* Kirit A. Bhatt, MD,*
Kenneth Wu, PhD,† Ivan N. Vial, BA,* Karine Padois, PhD,† Joshua M. Korman, MD,*‡, § and
Michael T. Longaker, MD, MBA*

Objective: To test the hypothesis that the mechanical environment of cutaneous wounds can control scar formation.

Background: Mechanical forces have been recognized to modulate myriad biologic processes, but the role of physical force in scar formation remains unclear. Furthermore, the therapeutic benefits of offloading cutaneous wounds with a device have not been rigorously tested.

Methods: A mechanomodulating polymer device was utilized to manipulate the mechanical environment of closed cutaneous wounds in red Duroc swine. After 8 weeks, wounds subjected to different mechanical stress states underwent immunohistochemical analysis for fibrotic markers. In a phase I clinical study, 9 human patients undergoing elective abdominal surgery were treated postoperatively with a stress-shielding polymer on one side whereas the other side was treated as standard of care. Professional photographs were taken between 8 and 12 months postsurgery and evaluated using a visual analog scale by lay and professional panels. This study is registered with ClinicalTrials.gov, number NCT00766727.

Results: Stress shielding of swine incisions reduced histologic scar area by 6- and 9-fold compared to control and elevated stress states, respectively ($P < 0.01$ for both) and dramatically decreased the histologic expression of profibrotic markers. Closure of high-tension wounds induced human-like scar formation in the red Duroc, a phenotype effectively mitigated with stress shielding of wounds. In the study on humans, stress shielding of abdominal incisions significantly improved scar appearance ($P = 0.004$) compared with within-patient controls.

Conclusions: These results indicate that mechanical manipulation of the wound environment with a dynamic stress-shielding polymer device can significantly reduce scar formation.

The ability to alter the outcome of a healing wound remains a fundamental goal of regenerative medicine. All adult human wounds heal with some degree of scar formation that compromises function and appearance after the estimated 230 million major surgical procedures performed worldwide each year.[1, 2] Importantly, none of the currently available approaches used to reduce postsurgical scarring (including ointments, tape, silicone sheeting, laser, and steroid injections) have substantial clinical efficacy,[3] thus emphasizing the need for better approaches to impact scar pathogenesis.

Studies in scarless repair during early mammalian gestation have provided important insight into putative fibrogenic mechanisms including inflammatory signaling and extracellular matrix composition.[4] A less-studied but equally relevant factor may be the mechanical environment, as significantly lower levels of mechanical stress are present during scarless fetal repair.[1,5] The importance of mechanical forces in scar formation is suggested by a wealth of preclinical and clinical data demonstrating exuberant scarring in anatomical areas with the highest levels of mechanical stress.[6,7] A unifying feature of the biological response to mechanical force is the production of load-bearing elements such as matrix components.[5,8,9] It remains unknown whether the attenuation of these mechanical cues may minimize the fibroproliferative response driving scar formation.

After injury, the principal load-bearing components of the skin must be rebuilt whereas physiologic stresses are actively imposed on the wound. If the newly formed structures, such as stress fibers within cells and matrix deposition in the extracellular space, cannot support the physiologic stresses, force equilibrium across the wound cannot be satisfied. As with any other material under these nonequilibrium conditions, the immature scar either ruptures (dehiscence) or gradually spreads (creep) over time. In living tissues such as skin, however, creep is characterized by hypertrophy of the underlying scar, suggesting an active biologic process.[10] Motivated by these observations, we examined the extent to which decreasing the mechanical stress across healing wounds with a novel device could promote healing without scar formation.

METHODS

Polymer Materials

Stress-shielding devices were manufactured using silicone polymer sheets (NuSil, Lafayette, CA) and pressure-sensitive adhesive (NuSil) secured to Teflon extension sheets (Dupont, Wilmington, DE) to obtain 40% prestrain. This produced a 20% compressive stress-shielding effect postapplication.

Animals

Studies were performed on adult purebred red Duroc swine (n = 6) in accordance with Stanford University animal guidelines. General inhalational anesthesia and sedation were provided by the veterinary staff. Full-thickness incisional or excisional wounds were

created on the pig dorsum and closed with 4-0 nylon sutures removed on day 4. Treatment wounds were stress-shielded immediately after closure. The stress-shielding devices were replaced on day 4 and weekly thereafter. Custom-designed pig jackets were used to protect the wounds and stress-shielding devices.

Strain Studies on Porcine Skin

We measured the stress versus strain behavior of unwounded 1 × 6 cm full-thickness pig skin samples. The linear portion of the stress-strain curve at low strains was used to determine Young's modulus. To determine the precise strain after application of the device, we stamped a standard grid (1 × 1 cm boxes) on unwounded skin. The engineering strains were calculated by measuring the change in dimension of the grid boxes.

Biomechanical Analysis of Porcine Wounds

By making parallel lines on unwounded skin, we were able to observe the line displacements after closure of the excised wound to directly measure local skin strain. Mechanics stress analysis was performed by mapping the in-plane stress and strain state by digital imaging. During wound closure, we used established computation image analysis with statistical error analysis of full-field displacements. Computational finite element analysis using nonlinear 3-dimensional analysis was performed to model the mechanical stress state.

Porcine Hypertrophic Scar Models

On each side of the pig dorsum, 5 wounds were placed in 1 row separated by 2.5 cm each, resulting in 10 wounds per animal. Treatment and control wounds were randomized to location, with equal distribution of wounds on either side of the dorsal midline and with respect to rostral or caudal positioning. Two surgical models were developed to increase tension across closed incisions:

1. Incisional wounds (3 cm) were subjected to stress shielding, elevated stress, or physiologic stress for 8 weeks. Elevated stress was generated by placing the devices on either side of the long axis of the incision in a "para-" position.
2. Full-thickness, oblate hexagonal excisions of increasing dimensions (length × width = 3 × 1 cm^2, 3 × 2 cm^2, 4 × 3 cm^2, or 5 × 3 cm^2) were created to increase wound tension after closure. We also created 3 × 1.5 cm^2 excisional wounds that were sutured closed and then either left unshielded or stress shielded for 8 weeks with the polymer device.

Histomorphometry

Full-thickness scars were harvested at 8 weeks and fixed in 4% paraformaldehyde before paraffin processing. For immunofluorescence, sections were incubated overnight with goat anti-pig CD31 (vascular density, Santa Cruz Biotechnology, Santa Cruz, CA) or rabbit anti-pig α-smooth muscle actin (Abcam Inc, Cambridge, MA) followed by rabbit antigoat FITC (Abcam Inc) or goat ant-irabbit Cy3 (Abcam Inc), and mounted with DAPI Vectashield (Vector Labs, Burlingame, CA). For light microscopy, sections were incubated overnight with rabbit anti-pig TGF-β1 (Santa Cruz Biotechnology) followed by goat anti-rabbit HRP (Abcam Inc). Sections were developed with diaminobenzidine (Vector Labs) and counterstained with hematoxylin. TGF-β1 intensity was scored on a scale from 0 (no signal) to +3 (strong signal). Image quantification by 2 blinded observers of at least 5 high-power fields was performed on the scar/wound/granulation tissue region using ImageJ (National Institutes of Health, Bethesda, MD).

Clinical Study

The study was undertaken between October 2008 and November 2009 with patients undergoing an elective abdominoplasty procedure. The study population excluded pregnant women, patients with a history of keloid disease, patients with any medical disorder or on any medication that could affect wound healing, or allergies to adhesives or medical tape. Study protocols were approved by an independent review board and performed in accordance with the Declaration of Helsinki and the International Conference on Harmonisation: Harmonised Tripartite Guidelines for Good Clinical Practice. Informed consent was obtained after the nature and possible consequences of the study were explained. At each patient visit, we assessed for adverse events and local toleration of the dressing. Safety parameters were assessed every week until the end of the study. Professional photographs were obtained under reproducible conditions by the same photographer between 8 and 12 months postsurgery and used for panel evaluation. This study is registered with ClinicalTrials.gov, number NCT00766727.

Scar Assessments

Two independent external panels (3 lay volunteers or 3 board-certified plastic surgeons) blinded to treatment assessed scar outcomes using 2 analyses: unpaired digital photographs of both treated and control incisions were randomly ordered and scored using a visual analog scale (VAS, 0-100 points),[11] and paired photographs were evaluated by reviewers who were asked to select the wound with less scar formation.

Statistical Analysis

Data are presented as mean ± SEM. For the porcine data, we used ANOVA with post hoc Tukey's HSD. For the clinical data, the primary outcome was VAS score and Wilcoxon signed-rank test was used to compare differences between paired stress-shielded and unshielded wounds. Continuous variables were evaluated using Pearson's correlation coefficient. All hypothesis tests were 2-tailed and the level of significance was set at $P < 0.05$.

RESULTS

Development of a Novel Stress-shielding Polymer to Control Skin Mechanics

A systematic evaluation of the role of mechanical forces on wound repair was first conducted in purebred red Duroc pigs, which are a robust model of overhealing analogous to human pathology.[12] To precisely control the wound mechanical environment, we developed a novel device with mechanical compliance similar to skin that would adhere to the outer layer of skin and provide uniform compressive strains across the wounds. The magnitude of the strains depended on the physiologic skin stress and the deformation properties of the skin.

The device consisted of a flexible polymer sheet with a high elastic recovery force and pressure-sensitive skin adhesive, capable of stress-shielding wounds during the critical phases of wound healing. The device was in a prestretched configuration before placement on the skin (Fig. 1A-B). After adhesion to the skin, device contraction was initiated, with the extent of contraction and the peri-wound strain state carefully controlled by the device thickness, mechanical properties and initial elastic prestrain. Because the device is transparent, markings on the underlying skin could be directly observed and measured to determine the imposed strains (Fig. 1C). Compressive strains of approximately 20% were applied after device contraction to ensure unloading of the physiologic wound stress.
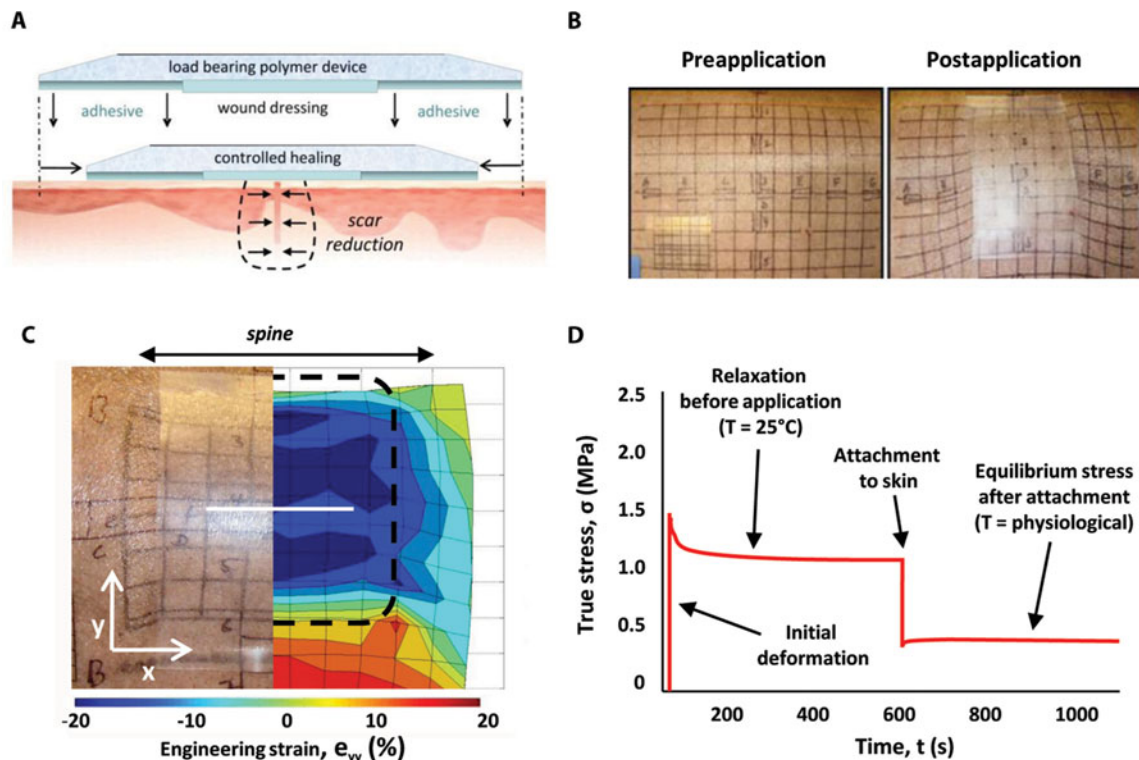
FIGURE 1. Development and testing of the stress-shielding polymer device in swine. **(A)** The stress-shielding device consists of a high elastic recovery force polymer attached to the skin surface in a prestretched configuration using a pressure sensitive adhesive. **(B)** Photographs of skin grid markings before and after polymer device application allow characterization of grid deformation and local skin stresses imposed by the mechanical force-modulating polymer. **(C)** The underlying skin strains were directly characterized by measurement of the deformation of an inked grid lateral to the dorsal midline (left). By proper selection of the prestretched device strain, the skin strains across the wound could be precisely controlled (right) and were consistent with finite element modeling where blue represents the reduced (compression) strain imposed and red represents the increased (tensile) strains. The black dotted line represents the outline of the stress-shielding device. **(D)** Skin strains were determined immediately before application, during attachment to skin, and after attachment to skin to ensure minimal polymer device viscoelastic relaxation for up to 12 weeks (with the device being replaced weekly).

To achieve this controlled strain state, both viscoelastic creep relaxation of the polymer material associated with prestraining and viscoelastic recovery after device attachment and deployment need to be accounted for (Fig. 1D). We carefully assessed creep deformation in the polymer backing, pressure-sensitive adhesive, and skin for up to 12 weeks to ensure that strains were accurately maintained ($\pm 5\%$ change in strain). Devices were deployed over incisions at the time of suture removal and weekly thereafter for 8 weeks.

Controlling Mechanical Stress Across Incisions in Red Duroc Pigs Regulates HTS Formation

One natural corollary of our hypothesis is that increasing physiologic stress across an incision should promote scarring as we had previously described in a small animal model.[5] To confirm this, we first developed a closed incisional model, which took advantage of the tensile stresses that are induced in skin adjacent to the stress-shielding device (Fig. 2A). Full-thickness incisional wounds were created and closed, and sutures removed on postoperative day 4 before treatment. By deploying devices on both sides of an incisional wound ("para" position) after suture removal, the forces across the wound were increased (elevated exogenous stress). We also stress-

shielded incisional wounds after suture removal by placing the device directly over the wound.

Altering skin stresses dramatically regulated the extent of scarring observed on gross or histologic examination. Importantly, incisional wounds under stress-shielding conditions (0.44 ± 0.12 mm^2) demonstrated nearly scarless closure with a 6- and 9-fold decrease in histologic scar area compared to control physiologic stress (2.53 ± 0.06 mm^2, $P < 0.01$) and elevated stress incisional wounds (3.96 ± 0.62 mm^2, $P < 0.01$), respectively (Fig. 2B-C). These differences were highly significant and demonstrate the ability to manipulate incisional scar formation through exogenously applied mechanical forces.

Stress Shielding of Porcine Wounds Prevents Expression of a Fibrotic Phenotype

Next, we analyzed surrogate markers that are increased in fibrosis and scar formation.[13,14] Comparisons were made between normal unwounded skin, non–stress-shielded incisions (physiologic stress), stress-shielded incisions, and incisions with elevated stress with respect to cellular density, blood vessel density (CD31), and α-smooth
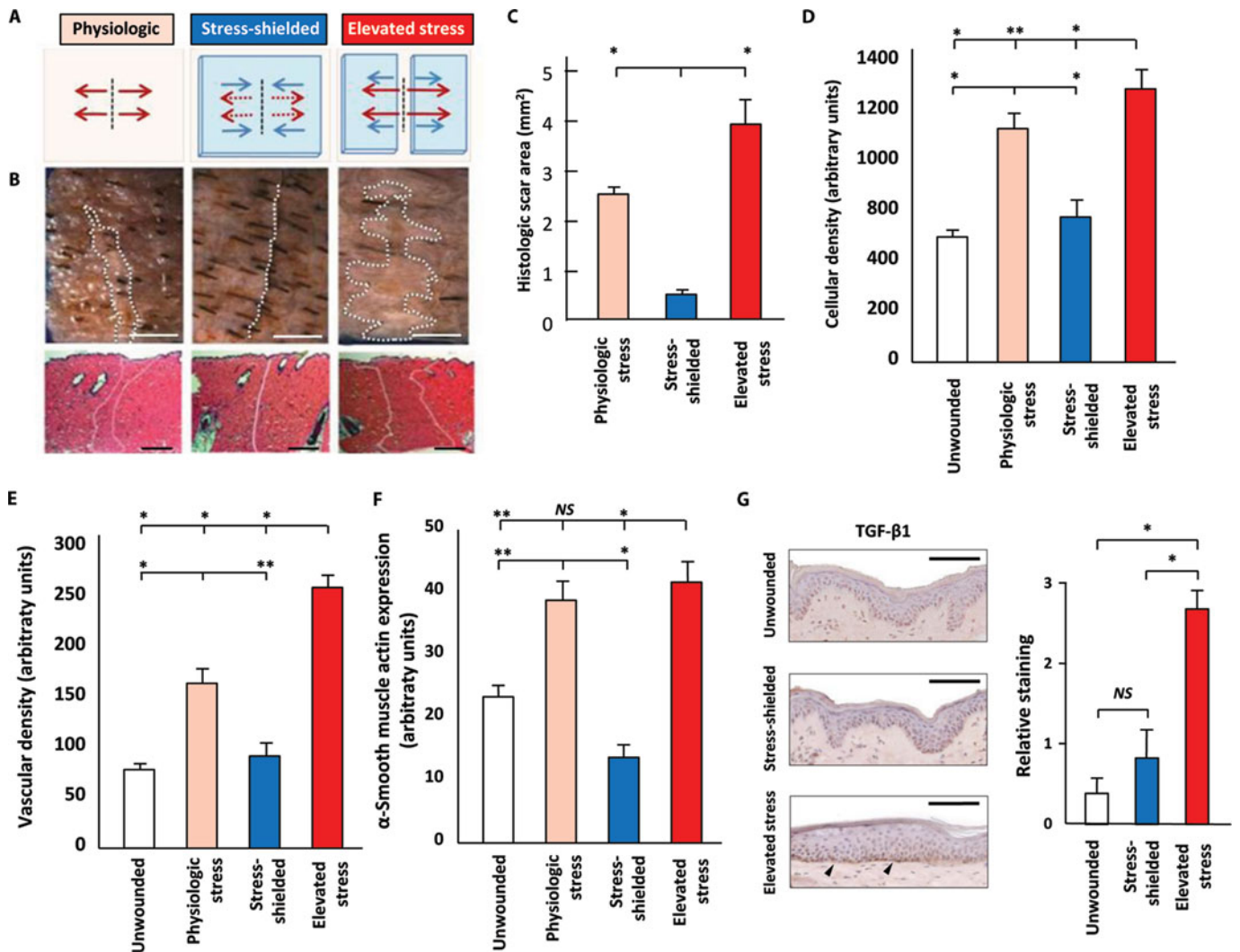
FIGURE 2. Modulation of mechanical stresses across porcine incisions controls the degree of scar formation. **(A)** Schematics of different stress states in incisional wounds. **(B)** The control wound (first column) that experienced physiologic skin stress is compared to the stress-shielded incision (second column) and the incision with elevated stresses (third column) obtained with para-positioned devices that increased stress on the healing incision. The white dotted lines (top row) outline surface scarring and correlate with the histological scar area (outlined in white, bottom row). **(C)** There is nearly a 9-fold reduction in scarring from the elevated stress to the stress-shielded wounds. **(D-F)** Quantification of fibrotic markers: cellularity (DAPI), vascularity (CD31), and α-smooth muscle expression in the different wound conditions. **(G)** Representative micrographs and semiquantitative analysis of TGF-β1 immunohistochemistry (brown color, arrowheads) at 8 weeks post-injury. Scale bar = 2000 μm (B, top row), 1000 μm (B, bottom row), and 50 μm (G). n = 5 wounds for each biomechanical condition. *$P < 0.01$; †$P < 0.05$.

muscle actin expression (Fig. 2D-F). All markers increased with tension and significantly decreased to levels similar to unwounded skin with stress shielding. Even at 8 weeks postinjury, mechanically stressed scars continued to exhibit strong profibrotic signaling at the epidermal-dermal junction, with stronger transforming growth factor-β1 (TGF-β1) immunoreactivity (2.7 $\pm$ 0.2, range: 0 = no signal to 3 = strong signal) compared to minimal signal in unwounded (0.3 $\pm$ 0.2, $P < 0.001$ relative to elevated stress) and stress-shielded wounds (0.8 $\pm$ 0.3, $P < 0.001$ relative to elevated stress) (Fig. 2G). The histomorphologic properties of unwounded skin directly under the stress-shielding polymer were not significantly different from distant unwounded skin regions, indicating that the applied stresses were not

sufficient to modify normal skin properties at these experimental time and force scales.

Mechanical Stress Levels Correlate With the Degree of Skin Fibrosis After Excisional Wound Closure in the Red Duroc Pig

To test the role of endogenous mechanical forces, we created excisional wounds of increasing size (3 $\times$ 1 cm^2, 3 $\times$ 2 cm^2, 4 $\times$ 3 cm^2, 5 $\times$ 3 cm^2), knowing that larger excisions would generate greater mechanical tension after closure (Fig. 3A). After the creation of full-thickness excisions, wounds were closed and sutures removed

after 4 days. Eight weeks post-injury, there was a significant amount of incisional scar formation (on gross and histologic evaluation) that positively correlated with the degree of tension after wound closure (Fig. 3B).

Stress Shielding of Porcine Wounds Promotes a Regenerative "Scar-free" Phenotype

Having demonstrated the role of both endogenous and exogenous mechanical forces to promote incisional scarring, we next addressed the challenge of whether the device could be used to reduce scarring in 3×1.5 cm^2 excisional wounds that were sutured closed under elevated skin stresses caused by wound closure itself (Fig. 4A). Sutures were removed on postoperative day 4 immediately before either stress-shielding treatment ("stress-shielded") or closed excisions were left unshielded ("elevated stress"). The ability of the device to reduce strain across the closed incision was measured in 3 experimental wound groups. Evaluation of strains revealed augmented tension strains ($+25 \pm 4\%$, $P < 0.01$ relative to unwounded) in the unshielded wounds and reduced tension strains ($-22 \pm 6\%$, $P < 0.001$ relative to unwounded) in the stress-shielded wounds (Fig. 4B). Once again, stress shielding dramatically decreased incisional scar area compared to elevated stress wounds (4.96 ± 0.97 mm^2 vs 14.94 ± 2.87 mm^2, $P < 0.01$) (Fig. 4C). Stress-shielded wounds also exhibited regeneration of unwounded epithelial architecture (Fig. 4A, left and right columns). In contrast, the unshielded wounds demonstrated classic features of hypertrophic scarring with increased cell density, epithelial thickening, and loss of rete pegs (Fig. 4A, middle column). Therefore, in addition to simply reducing the volume of fibrosis, the device seemed to promote regenerative-like repair rather than scar formation.

Stress Shielding of Human Wounds Significantly Reduces Scar Formation

The data from our pig experiments were highly compelling and are important from a translational perspective because swine skin is considered the closest to human skin for animal studies.[12] Given the promising preclinical results demonstrating the ability to control scar formation by manipulation of mechanical forces in postsurgical wounds, we tested our hypothesis in human patients. Specifically, we aimed to determine whether our dynamic stress-shielding device could significantly reduce postsurgical scarring in human wounds. To mimic the experimental conditions utilized in our red Duroc model, patients were enrolled who were undergoing a surgical procedure involving closure of large soft tissue excisions. These abdominoplasty procedures result in incisions closed under a large amount of tension (Fig. 5A), analogous to the closed excisional wound conditions in the pig model (Figs. 3–4). The scars that develop in these human wounds are prone to hypertrophy and spreading, thus providing a rigorous test to our hypothesis that stress shielding of mechanical forces would decrease postsurgical scarring.

The initial study population consisted of 10 healthy female adults with no significant medical comorbidities undergoing an elective abdominoplasty procedure. One patient exited the study early for non–device-related reasons and was excluded from the data analysis. The mean patient age was 40 years (range, 26–53 years) and the mean body mass index was 25.4 kg/m^2 (range, 19-31). Two patients had a history of cigarette smoking. Other patient demographics are shown in Table 1. The operations were performed by a single surgeon (J.M.K.) at a single center. The abdominal skin incision was closed with intradermal (under the skin surface) dissolvable sutures. Postoperatively, the entire abdominal incision (range, 28-36 cm) was left without any additional treatment until 8 days postoperatively (range, 4-14 days) when patients were seen in follow-up clinic. The incisions

were divided into left and right halves and randomly assigned to either stress-shielding treatment or control (no treatment). Patients were seen weekly for study monitoring and device changes for a minimum of 7 weeks.

Stress-shielding of human wounds resulted in a dramatic and significant reduction in scar formation when compared to within-patient control incisions (Fig. 5B). The lay panel scored scar appearance of stress-shielded wounds 13.2 points (range, 5.1-24.1 points, $P = 0.004$) better compared with control incisions (Fig. 5C), based on a validated VAS scale of 0 to 100 points.[11] The expert panel of 3 plastic surgeons unrelated to the study scored scar appearance of treated incisions 31.9 points (range, 12.7-48.0 points, $P = 0.004$) better compared with control incisions (Fig. 5C). The stress-shielded wound was never selected as worse and rated better compared with control in almost 95% of cases (51 of 54). No significant correlation between expert VAS score and either patient age ($R = 0.2$), body mass index ($R = 0.003$), or duration of device wear ($R = 0.1$) was detected. Patient ethnicity (white vs non-white, $P = 0.3$) did not significantly affect improvement in stress-shielding.

The use of the polymer devices was not associated with any significant adverse effects including wound dehiscence or delayed healing. Of the 93 recorded device applications, 89 (96%) were rated as comfortable and 0 (0%) peeled off prematurely. There was 1 complication of superficial soft tissue infection unrelated to device use that required outpatient treatment with oral antibiotics.

DISCUSSION

The enormous biomedical burden of fibroproliferative disease underscores the critical need for novel targeted therapies to both treat and prevent skin fibrosis.[15–17] Before effective treatments can be developed; however, an improved understanding of fibrogenic mechanisms is necessary. The role of mechanical force is increasingly being recognized in scar pathophysiology, and computer modeling studies have predicted that mechanical tension drives pathologic scarring in humans.[7,18] Furthermore, the use of negative pressure wound therapy has been anecdotally associated with scar formation,[19] supporting our findings that mechanical force can induce fibrotic repair.

Current clinical therapies to treat fibrosis are largely nontargeted approaches to pathway-specific processes. Treatment modalities such as surgical excision, steroid injections, and laser and radiation therapy are generally expensive, cumbersome, painful, and/or ineffective.[3] Several noninvasive therapies have demonstrated efficacy, which may be related to their manipulation of mechanical forces (eg, pressure garments, silicone sheeting, paper tape), although rigorous studies in this context are lacking.[20–23] Moreover, none of these approaches achieve precise control over the wound stress or strain state over extended periods, and most importantly, none have demonstrated a robust reduction in postsurgical scarring.

More recently, investigators have attempted biologic approaches to prevent HTS formation. A recent phase I/II trial used injected recombinant active TGF-β3 (an antifibrotic cytokine) to abrogate scar formation and demonstrated a 5- to 16-point improvement in VAS score.[24] These studies were performed in small (1 cm) incisions and required intradermal injections that caused some edema and erythema, raising concerns for immunologic reactions and potential disease transmission. In contrast, our clinical results with a novel stress-shielding device demonstrated a significant improvement (up to 32 VAS points) in scar appearance after the closure of large excisional defects that both laypersons and experts easily detected.

However, this is a preliminary clinical study with a limited number of patients that was designed to demonstrate proof of principle in humans. Larger clinical trials are being planned to include greater ethnic diversity within the patient population and to determine
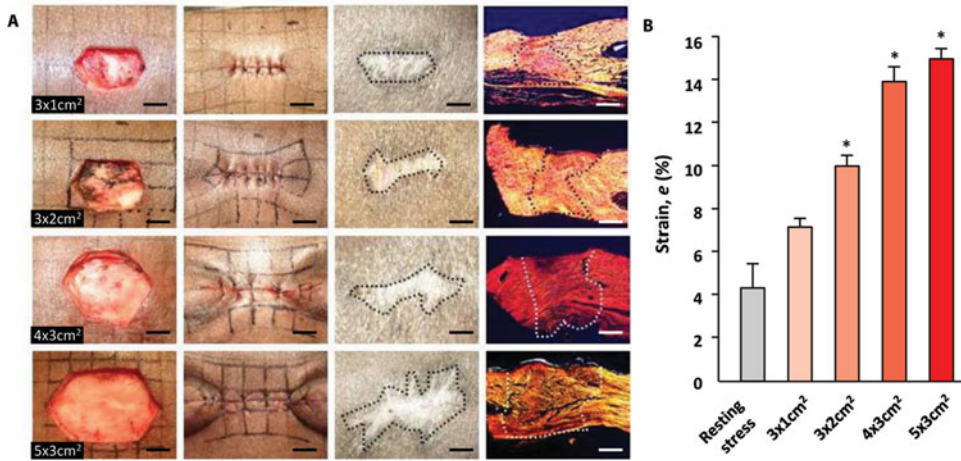
FIGURE 3. Wound stress levels correlate with degree of fibrosis. **(A)** From top to bottom, wounds of increasingly larger dimensions (3×1 cm^2, 3×2 cm^2, 4×3 cm^2, 5×3 cm^2) were created to generate incremental skin stresses (first column). Once sutured closed, the larger the excisional wound, the greater the strain levels (second column). Increased stress levels correlated with greater surface fibrosis (third column) and histologic fibrosis as seen on polarized light images (fourth column). **(B)** Measured strain levels were significantly elevated with increasing wound dimensions. Scale bar $= 10$ mm. *$P < 0.05$.
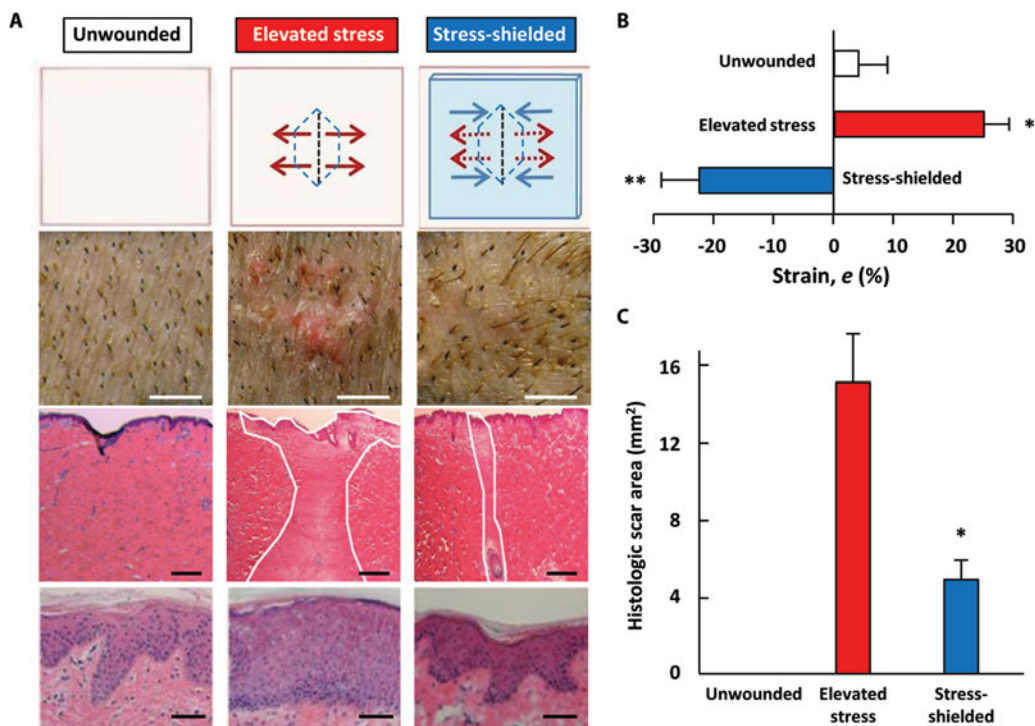
FIGURE 4. Dynamic stress shielding of high-tension incisions promotes skin regeneration. **(A)** Stress shielding of high-tension incisions (after closure of excisional 3×1.5 cm^2 wounds) resulted in dramatic reduction in scar formation. Unwounded (left column) skin is compared to the unshielded high-tension incisions, which experienced elevated skin stresses (middle column) and the stress-shielded high-tension incisions (right column). In the unshielded high-tension incisions, there was significant scarring in the dermis and significant hypertrophy of the epithelial layer (middle column) as seen in human hypertrophic scarring. In contrast, the stress-shielded wounds healed with no evidence of a scar, minimal dermal fibrosis on histology, and an epithelial layer resembling unwounded skin (right column). **(B)** Compressive strains of 20% were achieved with the dynamic stress-shielding polymer to offset elevated wound tension. **(C)** The stress-shielded high-tension incisions demonstrate a 3-fold reduction in histologic scar area compared to nonshielded high-tension incisions. Scale bar $= 5$ mm in second row A, 500 μm in third row A, 50 μm in bottom row A. n $= 5$ wounds for each biomechanical condition. *$P < 0.01$; †$P < 0.001$.
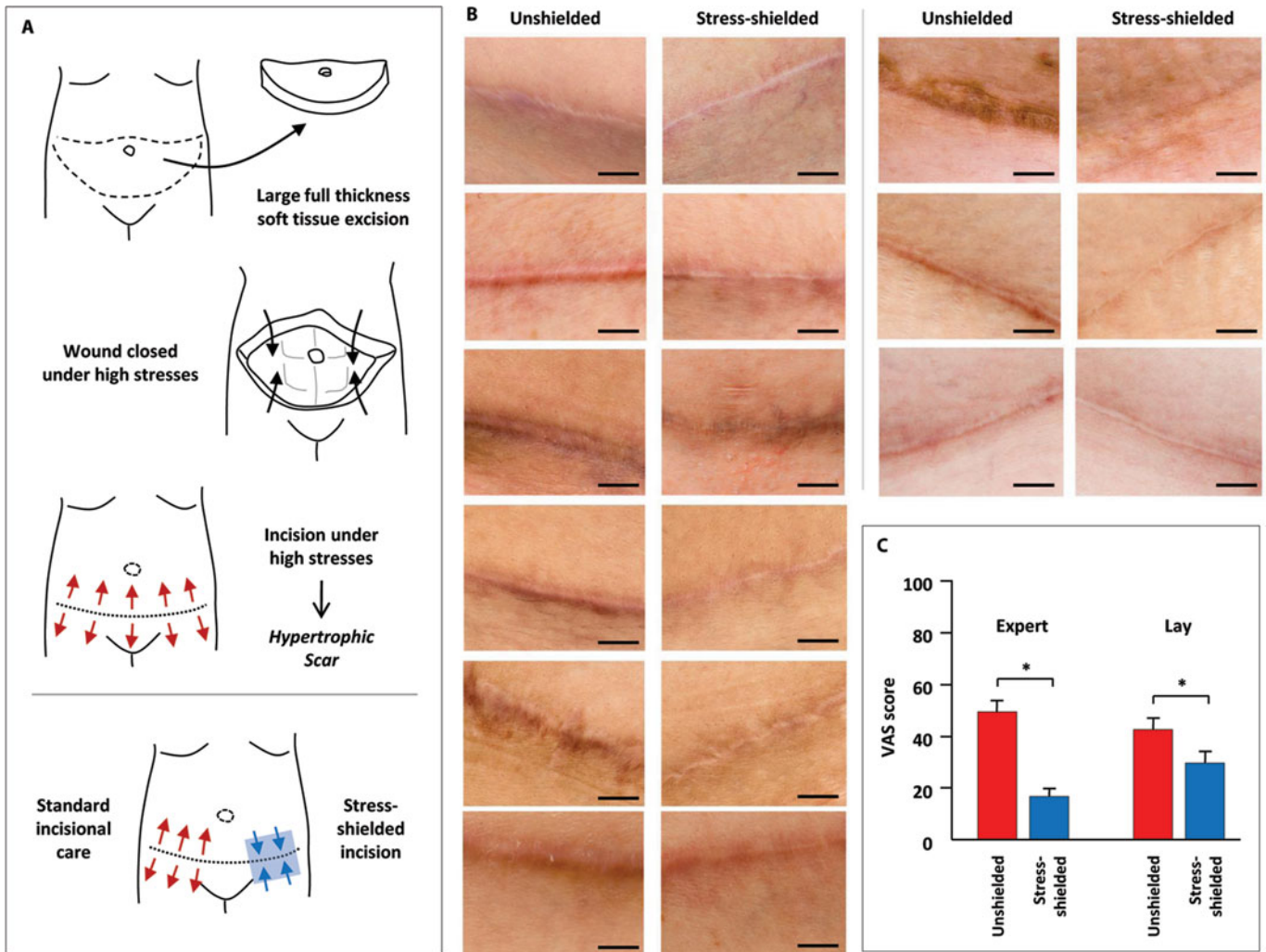
FIGURE 5. Stress shielding significantly reduces scar formation in human postsurgical incisions. **(A)** Abdominoplasty procedures involve the excision of an extensive amount of soft tissue (full-thickness skin and subcutaneous fat), which results in a high-tension (red arrows) incisional wound after closure with sutures. We hypothesize that these forces predispose wounds to HTS formation and that off-loading of mechanical stresses within abdominal incisions with a dynamic stress-shielding polymer will dramatically reduce scar formation. **(B)** Photographs of paired within-patient abdominal incisions at 6 to 12 months postsurgery (paired rows). Note the scar widening, elevation, irregularity, and discoloration in unshielded control incisions (left columns) compared with stress-shielded incisions (right columns). **(C)** Evaluation of professional photographs by both a lay panel and an expert panel demonstrated a significant improvement in scar appearance based on VAS scoring. Scale bar = 1 cm. *$P < 0.01$.

the optimal range of stress-shielding forces for anatomic region- and dimension-specific wounds. In addition, different durations of postoperative device wear need to be examined to establish an optimal treatment period for stress shielding. Moreover, some wounds demonstrated a dramatic improvement in scar appearance when compared to within-patient controls, whereas other scars showed less remarkable improvement. This may be due to differences in the amount of tension applied after wound closure, with highest tension wounds likely benefiting the most from stress-shielding treatment. Other scar attributes that need to be examined in future studies include scar redness, height, degree of itching, and biomechanics—clinical parameters that may shed light on the influence of mechanical forces on wound vascularization, proliferation, nerve function, and scar matura-

tion, respectively. Finally, treatment with the stress-shielding polymer device will need to be directly compared with other antiscar modalities such as silicone sheeting, compression dressings, or paper tape to determine the true efficacy and cost benefits of stress shielding compared to current standard therapies.

In summary, the findings of these preclinical and clinical studies are consistent with the biomechanical premise that when mechanical equilibrium is not satisfied between physiological skin stress and load-bearing components of the wound, the biological processes of repair are continuously stimulated to increase the amount of scar tissue and limit tissue regeneration (Fig. 6). Our translational studies shed important and unique insight into scar pathogenesis and demonstrate the ability of mechanical forces to significantly modulate wound

TABLE 1. Patient Demographics

Patient No.	Age	Sex	Ethnicity	Body mass index	Height, m	Mean VAS Improvement (Range 0-100 points, Lay)	Mean VAS Improvement (Range 0-100 points, Expert)
1	53	F	White	28	1.65	24.1	43.4
2	42	F	American Indian/Alaska Native	19	1.70	5.1	30.3
3	36	F	White	27	1.60	8.1	12.7
4	39	F	White	27	1.70	23.6	15.4
5	41	F	Native Hawaiian/Pacific Islander	26	1.57	17.7	47.6
6	45	F	Asian	25	1.52	7.5	40.6
7	26	F	White	31	1.73	11.1	33.5
8	35	F	Asian	23	1.57	23.8	48.0
9	43	F	Hispanic	23	1.65	5.9	15.4
Mean (range)	40(26-53)	—	—	25.4(19–31)	1.63(1.52-1.73)	13.2(5.1-24.1)	31.9(12.7-48.0)
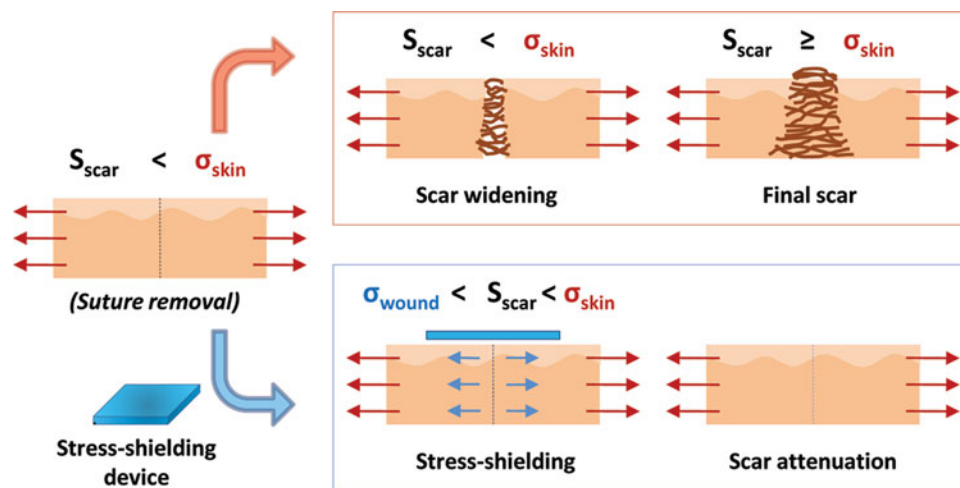
FIGURE 6. Biomechanical paradigm for hypertrophic scar formation. The schematic diagram demonstrates that after suture removal, the physiologic skin stress (σ_{skin}) overcomes the scar strength (S_{scar}) of the immature wound and causes increased fibrosis. This process continues until the scar strength of the mature scar is finally able to offset the physiologic skin stress (top right). Ideally, a stress-shielding device would counterbalance the physiologic skin stress to establish a mechanical environment whereby local wound stresses (σ_{wound}) are less than both wound strength (S_{scar}) and skin stresses (σ_{skin}) so that there would be no fibrosis (bottom right).

repair. We propose a biomechanical paradigm for wound regeneration whereby the mechanical environment of wounds, in addition to cellular, biochemical, and matrix components, must be precisely controlled to enable scarless tissue repair.

REFERENCES

1. Gurtner GC, Werner S, Barrandon Y, et al. Wound repair and regeneration. *Nature.* 2008; 453(7193):314–321.
2. Weiser TG, Regenbogen SE, Thompson KD, et al. An estimation of the global volume of surgery: a modelling strategy based on available data. *Lancet.* 2008; 372(9633):139–144.
3. Mustoe TA, Cooter RD, Gold MH, et al. International clinical recommendations on scar management. *Plast Reconstr Surg.* 2002;110(2):560–571.
4. Bullard KM, Longaker MT, Lorenz HP. Fetal wound healing: current biology. *World J Surg.* 2003; 27(1):54–61.
5. Aarabi S, Bhatt KA, Shi Y, et al. Mechanical load initiates hypertrophic scar formation through decreased cellular apoptosis. *FASEB J.* 2007;21(12): 3250–3261.
6. Wray RC. Force required for wound closure and scar appearance. *Plast Reconstr Surg.* 1983; 72(3):380–382.
7. Ogawa R. Keloid and hypertrophic scarring may result from a mechanoreceptor or mechanosensitive nociceptor disorder. *Med Hypotheses.* 2008;71(4): 493–500.
8. Desmouliere A, Chaponnier C, Gabbiani G. Tissue repair, contraction, and the myofibroblast. *Wound Rep Regen.* 2005;13(1):7–12.
9. Derderian CA, Bastidas N, Lerman OZ, et al. Mechanical strain alters gene expression in an in vitro model of hypertrophic scarring. *Ann Plast Surg.* 2005;55(1):69–75.

© 2011 Lippincott Williams & Wilkins

10. Wilhelmi BJ, Blackwell SJ, Mancoll JS, et al. Creep vs. stretch: a review of the viscoelastic properties of skin. *Ann Plast Surg.* 1998; 41(2): 215–219.

11. Duncan J, Bond J, Mason T, et al. Visual analogue scale scoring and ranking: a suitable and sensitive method for assessing scar quality? *Plast Reconstr Surg.* 2006;118(4):909–918.

12. Ramos MLC, Gragnani A, Ferreira LM. Is there an ideal animal model to study hypertrophic scarring? *J Burn Care Res.* 2008;29(2):363–368.

13. Harunari N, Zhu KQ, Armendariz RT, et al. Histology of the thick scar on the female, red Duroc pig: final similarities to human hypertrophic scar. *Burns.* 2006;32(6):669–677.

14. Lee JYY, Yang CC, Chao SC, et al. Histopathological differential diagnosis of keloid and hypertrophic scar. *Am J Dermatopathol.* 2004;26(5): 379–384.

15. Aarabi S, Longaker MT, Gurtner GC. Hypertrophic scar formation following burns and trauma: new approaches to treatment. *PLoS Med.* 2007; 4(9):e234.

16. Wynn TA. Common and unique mechanisms regulate fibrosis in various fibro-proliferative diseases. *J Clin Invest.* 2007;117(3):524–529.

17. Wynn TA. Cellular and molecular mechanisms of fibrosis. *J Pathol.* 2008;214(2):199–210.

18. Akaishi S, Akimoto M, Ogawa R, et al. The relationship between keloid growth pattern and stretching tension: visual analysis using the finite element method. *Ann Plast Surg.* 2008;60(4).

19. Lee HJ, Kim JW, Oh CW, et al. Negative pressure wound therapy for soft tissue injuries around the foot and ankle. *J Orthop Surg Res.* 2009;4:14.

20. Macintyre L, Baird M. Pressure garments for use in the treatment of hypertrophic scars—a review of the problems associated with their use. *Burns.* 2006;32(1):10–15.

21. Mustoe TA. Evolution of silicone therapy and mechanism of action in scar management. *Aesthetic Plast Surg.* 2008;32(1):82–92.

22. Reiffel RS. Prevention of hypertrophic scars by long-term paper tape application. *Plast Reconstr Surg.* 1995;96(7):1715–1718.

23. Atkinson JA, McKenna KT, Barnett AG, et al. A randomized, controlled trial to determine the efficacy of paper tape in preventing hypertrophic scar formation in surgical incisions that traverse Langer's skin tension lines. *Plast Reconstr Surg.* 2005;116(6):1648–1656; discussion 1657–1658.

24. Ferguson MWJ, Duncan J, Bond J, et al. Prophylactic administration of avotermin for improvement of skin scarring: three double-blind, placebo-controlled, phase I/II studies. *Lancet.* 2009; 373(9671): 1264–1274.